Rescaling Retinal Size into Perceived Size: Evidence for an Occipital and Parietal Bottleneck

Sylvia Kreutzer[1], Ralph Weidner[1], and Gereon R. Fink[1,2]

Abstract

■ The spatial and temporal context of an object influence its perceived size. Two visual illusions illustrate this nicely: the size adaptation effect and the Ebbinghaus illusion. Whereas size adaptation affects size rescaling of a target circle via a previously presented, differently sized adaptor circle, the Ebbinghaus illusion alters perceived size by virtue of surrounding circles. In the classical Ebbinghaus setting, the surrounding circles are shown simultaneously with the target. However, size underestimation persists when the surrounding circles precede the target. Such a temporal separation of inducer and target circles in both illusions permits the comparison of BOLD signals elicited by two displays that, although objectively identical, elicit different percepts. The current study combined both illusions in a factorial design to identify a presumed common central mechanism involved in rescaling retinal into perceived size. At the behavioral level, combining both illusions did not affect perceived size further. At the neural level, however, this combination induced functional activation beyond that induced by either illusion separately: An underadditive activation pattern was found within left lingual gyrus, right supramarginal gyrus, and right superior parietal cortex. These findings provide direct behavioral and functional evidence for the presence of a neural bottleneck in rescaling retinal into perceived size, a process vital for visual perception. ■

INTRODUCTION

Vision is not a passive reception of the world outside, rather, it arises through active integration and interpretation of incoming signals. Visual illusions illustrate this nicely. For instance, the Ebbinghaus illusion shows how contextual information in the spatial domain influences perception: A central circle appears larger when it is surrounded by smaller inducer circles and smaller when it is surrounded by larger inducer circles (Jaeger & Pollack, 1977; Cooper & Weintraub, 1970). However, vision does not only integrate information across space but also over time, as indicated by another illusion—the size adaptation effect. There, a circle appears smaller when a larger "adaptor" circle precedes it and larger when it follows a smaller adaptor circle (e.g., Pooresmaeili, Arrighi, Biagi, & Morrone, 2013). Although both illusions rely on different types of information integration, both affect the perceived size of a target circle. Because of this common perceptual consequence, the two illusions are well suited to investigate whether and how different visual contextual illusions interact at the behavioral and neural level. Combining both illusions in a factorial manner (Figure 1) allows looking for shared mechanisms that underlie the rescaling of perceived size.

Behavioral and functional imaging studies indicate that illusory size information is available at early levels of visual processing (Plewan, Weidner, & Fink, 2012; Busch & Müller, 2004) and that illusory size is encoded as early as in primary visual cortex (V1) (Fang, Boyaci, Kersten, & Murray, 2008; Murray, Boyaci, & Kersten, 2006). This view is supported by findings demonstrating that functional and anatomical features of V1 predict participants' susceptibility to visual illusions (Schwarzkopf & Rees, 2013; Schwarzkopf, Song, & Rees, 2011). In addition, local inhibitory mechanisms within V1 directly contribute to size rescaling when it is induced by size adaptation (Pooresmaeili et al., 2013). However, there is also evidence that higher visual areas modulate the encoding of perceived size in V1. These presumably include the lateral occipital complex (LOC; Weidner & Fink, 2007) and retrograde injection of information from extrastriate areas within parietal (Bullier, 2001) and prefrontal (Libedinsky & Livingstone, 2011; Lumer & Rees, 1999) cortices. For instance, Weidner and Fink (2007) showed that illusion strength correlated with activity in LOC as well as in right superior parietal lobule (rSPL). However, repetitive TMS over LOC—but not rSPL—reduced illusion strength (Mancini, Bolognini, Bricolo, & Vallar, 2010). This suggests that only LOC is causally involved in illusion generation. Unlike LOC, right parietal cortex appears to encode illusory size only when it is task relevant (Plewan, Weidner, Eickhoff, & Fink, 2012). On the basis of these findings, LOC may constitute a central size-scaling module that transforms retinal into perceived size. In contrast, task-specific regions in parietal cortex might retrieve this information when required.

[1]Research Center Jülich, [2]Cologne University

Here, we aimed to identify such a putative central size-scaling module by combining the Ebbinghaus illusion and the size adaptation effect within the same experimental paradigm. Both generate illusory overestimation or underestimation of the perceived size of a target circle. To separate the inducers and the target stimuli, we presented them consecutively. For the size adaptation effect (in which the test stimulus appears after the illusion-inducing adaptor stimulus), this is easy to implement. In contrast, in the classical setting of the Ebbinghaus illusion, the surrounding inducer circles are presented at the same time as the central target circle. However, Jaeger and Pollack (1977) demonstrated that, when an Ebbinghaus illusion leads to an underestimation but not an overestimation, it persists for a successive presentation of inducers and targets. In the current study, we used this effect to establish a temporal separation of the illusion-inducing and target stimuli in the Ebbinghaus illusion as well. We combined the two illusions in a factorial design to manipulate simultaneously the perceived size of the same target circle thereby testing for common effects and potential interactions. The temporal separation ensured that the neural activations reflecting the physical properties of illusion-inducing stimuli and the neural activations associated with encoding perceived size could be separated.

Because of Jaeger and Pollack's (1977) asymmetry between overestimation versus underestimation of target size in the successive version of the Ebbinghaus illusion, we used size adaptation alone to increase perceived size. Size underestimation, on the other hand, was varied by size adaptation as well as the Ebbinghaus illusion. On the basis of our previous work (Weidner & Fink, 2007), we expected that the brain areas involved in processing common aspects of both illusions, including changes in perceived size, would be located in ventral visual areas, particularly in LOC. If a common capacity-limited size-scaling mechanism is responsible for the temporal illusion effects, we expect to find an interaction between the two illusions at the behavioral and neural level. A strength of the present design is that the interaction contrast with respect to changes of perceived size was orthogonal: Both types of adaptation (i.e., an increase or a decrease) can be compared conjointly to no adaptation, hence eliminating any net changes of perceived size. Moreover, because illusion-related information was relevant, rSPL (Weidner & Fink, 2007) was expected to be modulated by illusory information.

METHODS

Procedure

Participants were invited for two sessions—one training session and one session in the MRI scanner—during which they performed a size comparison task. The perceived size of circles was manipulated using the two visual illusions.

Participants

Twenty-five participants (13 women, mean age = 26.8 years, age range = 21–39 years) took part in the current study. No neurological or psychiatric disorder was reported. All participants had normal or corrected-to-normal vision and were right-handed as measured using the Edinburgh Handedness Inventory (Oldfield, 1971). Written informed consent was obtained before the experiment in accordance with the Declaration of Helsinki. Participants were remunerated for their time. The study was approved by the ethics committee of the German Society of Psychology.

MRI Session

MRI sessions lasted half an hour and consisted of 12 blocks with 12 trials each. Stimuli were presented on a 30-in. shielded LCD monitor (60 Hz) at a distance of 245 cm and were seen via a mirror system installed on top of the head coil. Each trial started with a 5-sec presentation of an adaptation display, which, after a variable ISI, was followed by a test display that appeared for 200 msec (Figure 1). This brief presentation time was essential for size adaptation and the temporally separated Ebbinghaus illusion as the illusion strength decreases with longer visual inspection time. Throughout the experiment, observers were asked to fixate a cross at the center of the screen.

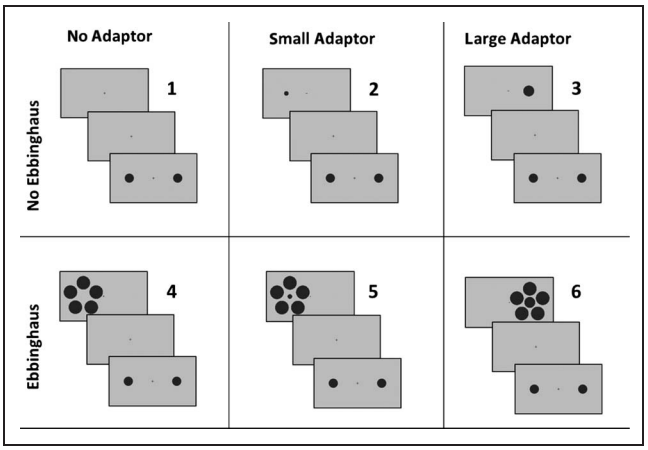

Figure 1. Stimuli and conditions. The figure depicts the trials of the six possible conditions. All trials started with a 5-sec presentation of the adaptation display, followed by a jittered ISI and a 200-msec presentation of the test display. There is no illusion in Condition 1. Conditions 2 and 3 illustrate the size adaptation effect where small (2) and respectively large (3) adaptor circles are presented first leading to an overestimation and underestimation, respectively, of the following test stimulus. Condition 4 shows the Ebbinghaus illusion where a set of large inducer circles is presented first leading to an underestimation of the test stimulus, which appears then in the center of this arrangement. In the classical Ebbinghaus illusion, the large inducer circles and the test stimulus are always presented simultaneously. Conditions 5 and 6 combine the Ebbinghaus illusion and the size adaptation effect.

Stimuli

Adaptation displays. The adaptation displays always lasted 5 sec. They consisted of either a single adaptor circle, a circular arrangement of Ebbinghaus inducer circles, or a combination of both (Figure 1). Stimuli consisted of gray circles presented on a medium gray background (35.5 cd/m^2). The circles flickered at a frequency of 4 Hz from light (69.6 cd/m^2) to dark (7.3 cd/m^2) gray. Flickering was added to prevent afterimages that could interfere with the two illusions (Sperandio, Lak, & Goodale, 2012). In a randomized manner, stimuli appeared 3° to the left (50%) or right (50%) of the fixation cross. The fixation cross had the same color as the circles and appeared at the center of the screen. The adaptor used for the size adaptation effect was either smaller (0.5°) or larger (1.0°) than the target (0.75°), and the circular Ebbinghaus inducer arrangement was composed of five large circles of a diameter of 0.9° spread out evenly at a radius of 2° from the center. Alternatively, during the neutral condition (illusion absent, no adaptor), the adaptation display was omitted, and only intertrial intervals (ITIs) and ISIs separated subsequent test displays. ISIs and ITIs were both jittered across trials within each block to allow for successful separation of the activation elicited by the adaptation and test displays. ISIs were, on average, shorter (ranging from 1.6 to 3.8 sec) than ITIs (ranging from 2.8 to 5 sec) to increase the statistical power of the design as estimated with the SPM software (Wellcome Department of Imaging Neuroscience, London, United Kingdom; www.fil.ion.ucl.ac.uk/spm/software/spm8).

Test displays. Test displays lasted 200 msec and always contained two circles, namely, the target and the probe. The target was always presented at the position of the prior adaptation display, and consequently, its size was presumed to be altered by the adaptation effect. Simultaneously, a probe circle appeared opposite to the adaptor and served as a reference stimulus unaffected by adaptation. The method of constant stimuli was used to ensure identical probe sizes across blocks, hence resulting in identical visual stimulation regarding test displays across conditions. Six probe sizes were determined for each participant individually based on the smallest (mean diameter = 1.13°, SD = 0.06°) and largest (mean diameter = 1.47°, SD = 0.08°) perceived size in a previous training session (see below). Both values were linearly scaled (factor = 1/1.8) to adjust sizes to the MRI setting and used to generate the six individual probe sizes: The smallest perceived size and the largest perceived size were extracted. On the basis of these, four additional values were determined: two values in between the smallest and largest perceived sizes and, at the same step size, one smaller than the smallest size and one larger than the largest size. The probe stimuli presented were identical across all experimental conditions. Note that, although every participant had six individual probe sizes, this did not affect the fMRI analysis as the conditions were compared within participants on the first level. Accordingly, in the contrasts entering the second-level analyses, activations induced by the probe stimuli canceled each other out.

Task and Design

A 2 × 3 factorial design combining the two independent variables Ebbinghaus inducers (present, absent) and Size adaptation (none, small and large adaptors) resulted in six possible adaptation displays. Adaptation conditions were kept constant within an experimental block, and each condition was presented in two blocks. Consequently, a session consisted of 12 blocks. The order of blocks was randomized. One block consisted of a maximum of 20 trials, and blocks were separated by breaks of 4 sec.

Instructions

During the test display period, observers had to indicate which of the two circles appeared either larger (15 observers) or smaller (10 observers) by pressing a button with their right index and middle fingers. In addition, a red-dot detection task was used to maintain the participant's attention on the preceding adaptation figure: During the adaptation display, a red dot (36.5 cd/m^2) appeared on the inducer or adaptor circles for 250 msec, and participants had to detect this dot as fast as possible by pressing a button. No red dot was shown during the neutral condition.

Data Analysis

The free statistical software R (R Foundation for Statistical Computing, Vienna, Austria; www.r-project.org) was used to analyze the behavioral data. The dependent variable perceived size was assessed by fitting a Gaussian function. The fitted parameters were used to identify the point of subjective equality (PSE; i.e., the point where both circles appear equal in size). PSEs were entered into a 2 × 3 repeated-measures ANOVA with factors Ebbinghaus illusion (present, absent) and Size adaptation (none, small, large). In addition, the accuracy in detecting the red dot was calculated.

Training Session

The training session was run between 1 and 6 weeks before the fMRI study and was implemented to familiarize participants with the task. Task and instructions during the training session were identical to those implemented during the MRI session later. During the training session, perceived target size was measured using the adaptive algorithm called parametric estimation by sequential testing (Macmillan & Creelman, 1991). The parametric-estimation-by-sequential-testing algorithm determines the PSE by sequentially varying probe size in response to the participants' answers. Stimuli were presented on a 22-in. Samsung

SyncMaster monitor (120 Hz) at a distance of 72 cm. Distance was preserved by a chin and forehead rest. Visual angles were linearly scaled (factor = 1.8) as compared with the fMRI setting.

MRI Data Acquisition and Analysis

Scanning parameters. A 3-T Trio MRI system (Siemens, Erlangen, Germany) was used to acquire functional imaging data. The images were collected by means of a T2*-weighted EPI sequence with a repetition time of 2.2 sec and an echo time of 30 msec. Eight hundred forty volumes of 36 axial slices each were measured with interleaved slice acquisition mode to obtain whole-brain coverage for every participant. Slice thickness was 3 mm with an inter slice distance of 15% (i.e., 0.4 mm). The field of view was 200 mm, using a 64 × 64 image matrix and resulting in a voxel size of 3.1 × 3.1 × 3.0 mm^2.

Preprocessing. Imaging data were preprocessed and analyzed using the SPM software. The first nine images that were acquired before the first stimulus appeared and before a steady BOLD signal was reached were omitted from further analysis. All images were realigned to correct for participant movements during scanning and normalized to the mean image as extracted with the segmentation function. Finally, data were smoothed using a Gaussian kernel of 8-mm FWHM.

Imaging data analysis. Two participants were excluded from analysis: one participant because of technical problems during the measurement and another participant because of abnormally high error rates (more than 2 *SD*s from the group mean). For the remaining data ($n = 23$ participants), six onset regressors representing the six experimental conditions were set up coding the time points when test displays appeared on the screen.

Trials involving the red dot, which was presented to keep participants' attention on the adaptors, were excluded from the analysis as full attention was not guaranteed and so were trials with missing responses. On average, 13.5% of the trials were discarded including the 10% of trials showing the red dot. The BOLD response was modeled using a canonical hemodynamic response function and its time derivative. Moreover, onset regressors for missing values, the red dot trials, and the six head movement parameters as well as the onset times of the adaptation displays were included as regressors of no interest in the model. Importantly, modeling the onsets of the adaptation displays separately facilitated analyzing the test displays independently. Initially, first-level contrasts for the six different conditions were specified by setting the regressor of interest to 1 and all other regressors to zero. Model estimation was performed using the ANOVA flexible factorial design as implemented in SPM8. Next, differential contrasts were calculated at the second level.

A conjunction analysis for the two main effects Ebbinghaus illusion and size adaptation effect was conducted. For both main effects, conditions with a smaller perceived size were subtracted from those with a larger perceived size: For the Ebbinghaus illusion, this meant subtracting activity for the Ebbinghaus illusion present trials (decreased perceived size) from activity for the Ebbinghaus illusion absent trials. For the size adaptation effect, activity after large adaptors (decreased perceived size) was subtracted from activity after small adaptors (increased perceived size).

The interaction of interest identified activations for Ebbinghaus absent versus present that differed depending on the simultaneous absence or presence of the size adaptor. In other words, the interaction aimed at identifying brain areas where processing one illusion was modified when the need arose to simultaneously process another illusion. All second-level contrasts are reported as t contrasts with a corrected threshold of $p < .05$ at the cluster level (resulting from $p < .001$ at the voxel level).

RESULTS

Behavioral Data

A 2 × 3 repeated-measures ANOVA with the factors Ebbinghaus inducers (present, absent) and Size adaptation (none, small, and large adaptors) was performed to analyze the PSEs (Table 1, Figure 2). To correct for violations of the assumption of sphericity, a Greenhouse–Geisser correction was conducted. Overall, two significant main effects and a significant interaction were found. Size adaptation did increase (small adaptor) and decrease (large adaptor) perceived size (main effect, Size adaptation: $F(2, 42) = 44.87$, $p < .0001$), and the Ebbinghaus

Table 1. Behavioral Data

	No Adaptor	*Small Adaptor*	*Large Adaptor*
No Ebbinghaus	1.00 (*SD* = 0.17)	1.14 (*SD* = 0.17)	0.68 (*SD* = 0.12)
Ebbinghaus	0.76 (*SD* = 0.20)	0.82 (*SD* = 0.17)	0.70 (*SD* = 0.10)

The table summarizes the perceived size of the target circle for all conditions. Perceived size is given as part of the true size and was derived from the PSE where participants responded at chance level and target and comparison circle size could no longer be discriminated. PSEs were derived by fitting a Gaussian function to the data. Assuming that the PSE for the neutral condition represents the true size, the perceived size for the other conditions was calculated.

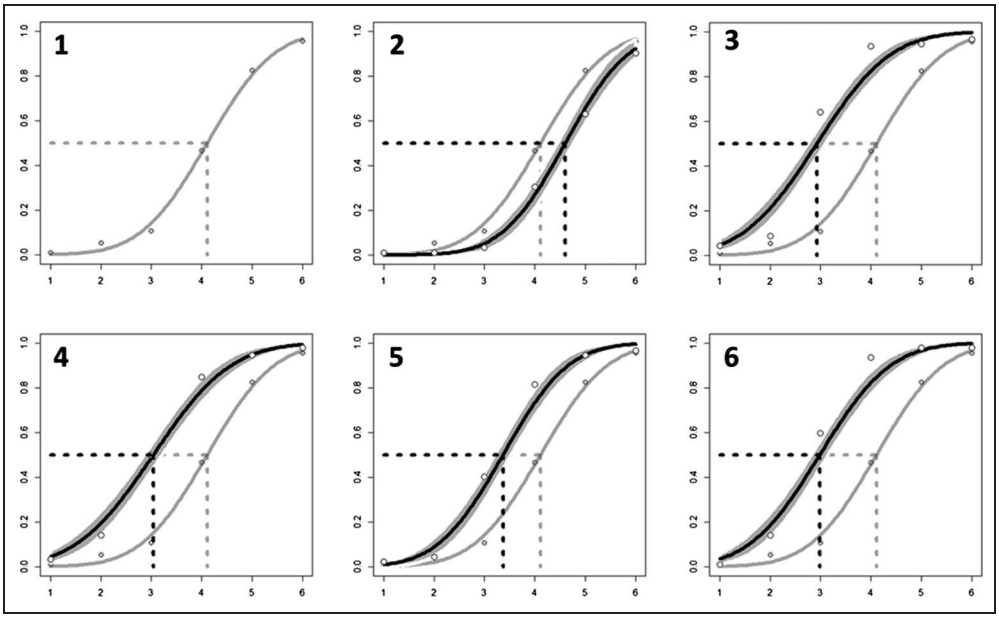

Figure 2. Behavioral data. The PSEs for all conditions across all participants (n = 23) during the experimental session are indicated by the dashed lines. The x axis represents the six comparison circle sizes (arbitrary units), which were derived from the behavioral pretest and therefore differed for all participants. Size judgment on the y axis reflects the portion of trials where the comparison appeared larger than the target circle. Thus, the more the black curve is shifted to the left compared with the neutral condition (gray), the more likely the comparison circle was to appear larger than the target, indicating decreased perceived size of the target.

illusion successfully decreased perceived size (main effect, Ebbinghaus illusion: $F(1, 21) = 65.14$, $p < .0001$). The decrease in perceived size did not add up for the combination of the Ebbinghaus illusion and the large size adaptor resulting in a significant interaction (interaction: $F(2, 42) = 20.92$, $p < .0001$). The same results were found in the training session during which adaptive testing was used rather than constant stimuli (main effect, Ebbinghaus illusion: $F(1, 30) = 72.82$, $p < .0001$; main effect, Size adaptation: $F(2, 60) = 78.69$, $p < .0001$; interaction: $F(2, 60) = 25.95$, $p < .0001$). This provides a replication of the two illusion effects as well as their interaction using two different psychophysical approaches.

In more detail, the main effect of the Ebbinghaus illusion reduced perceived size of the target from 0.93 to 0.75 averaged over the three size adaptation conditions, whereas the Ebbinghaus circles presented without an adaptor circle decreased perceived size to 0.76. Furthermore, perceived size was decreased to 0.82 when the Ebbinghaus circles were presented combined with the small adaptor. In combination with the large adaptor, the Ebbinghaus illusion reduced perceived size to 0.70. Multiple pairwise comparisons in form of Bonferroni corrected t tests (from here on referred to as pairwise comparisons) showed that these underestimations were all significantly different from the neutral condition and from the small adaptor presented alone. Investigating the size adaptation effect in more detail, the small adaptor (Ebbinghaus absent) increased perceived size to 1.14, whereas the large adaptor led to an underestimation of 0.68 when presented without the Ebbinghaus illusion. Pairwise comparisons showed that this underestimation was also significantly different from the neutral condition and the overestimation. The difference between overestimation and the neutral condition was only marginally significant ($p = .06$, $df = 22$).

Finally, the significant interaction between the two illusions revealed that the underestimations caused by the Ebbinghaus stimuli per se (without an additional adaptor) were not further modulated by adding a large adaptor ($p = 1.0$, $df = 22$). In addition, both illusion effects were not significantly different from adaption effects induced solely by a large adaptor (without Ebbinghaus stimuli; $p = 1.0$, $df = 22$ and $p = 1.0$, $df = 22$) as shown by pairwise comparisons. Hence, the underestimation as caused by the two illusions neither differed nor added up, suggesting that there is an upper limit in size scaling capacity and that the mechanisms involved in generating both illusions draw on these finite capacities.

Mean accuracy in detecting the red dots was 75.56%. Furthermore, the size judgment task was performed well as indicated by low miss rates of 6.28% on average. Mean RTs for the size judgment ranged from 368.25 to 752.11 msec (mean = 564.82 msec, SD = 110.11 msec).

Functional Imaging Data

Perceived Size

Activation during larger perceived size minus activation during smaller perceived size was investigated by a conjunction analysis of both illusions. The global conjunction analysis in SPM8 reveals voxels where both illusions cause consistently high activation changes in the same direction and are jointly significant. It should be noted that a significant conjunction indicates that one or more effects were present (Friston, Penny, & Glaser, 2005). This analysis aimed at identifying areas of activation because of changes in perceived size regardless of the type of illusion. The global conjunction analysis of the two illusions identified three significant clusters (Table 2a, Figure 3). First, a cluster of activation was observed in the right occipital lobe,

Table 2. Overview of fMRI Results

Contrast	*Region*	*Cluster Size*	*Side*	*x*	*y*	*z*	*Z Score*
(a) Conjunction: Ebbinghaus absent > present; small adaptor > large adaptor	Fusiform gyrus	641	R	32	−76	−10	5.22
	Cuneus	715	L	−10	−98	16	3.14
	Inferior frontal gyrus	149	L	−52	20	30	2.85
(b) Interaction: Adaptor present/absent × Ebbinghaus illusion present/absent	Supramarginal gyrus	428	R	54	−22	24	4.62
	Lingual gyrus	440	L	−14	−66	0	4.44
	SPL	214	R	24	−44	52	4.30

Coordinates were defined within Montreal Neurological Institute space. Activations were all significant at $p < .001$ (uncorrected), with an extent voxel threshold that allows including the number of voxels of the smallest significant cluster at $p < .05$ (family-wise error). L = left; R = right.

spreading from the fusiform gyrus to the inferior, middle, and superior occipital gyri and medially into the calcarine sulcus. Contralaterally, a similar cluster was found expanding from the cuneus to the lingual gyrus and the superior occipital gyrus. In addition, a cluster was found around the left inferior frontal gyrus (IFG, pars triangularis) corresponding to Brodmann's area (BA) 45 (probabilities for maximum 1: 50%, maximum 2 and 3: 70%) and BA 44 (probabilities for maximum 1: 30%, maximum 3: 40%) as indicated by the SPM Anatomy toolbox (Eickhoff et al., 2005).

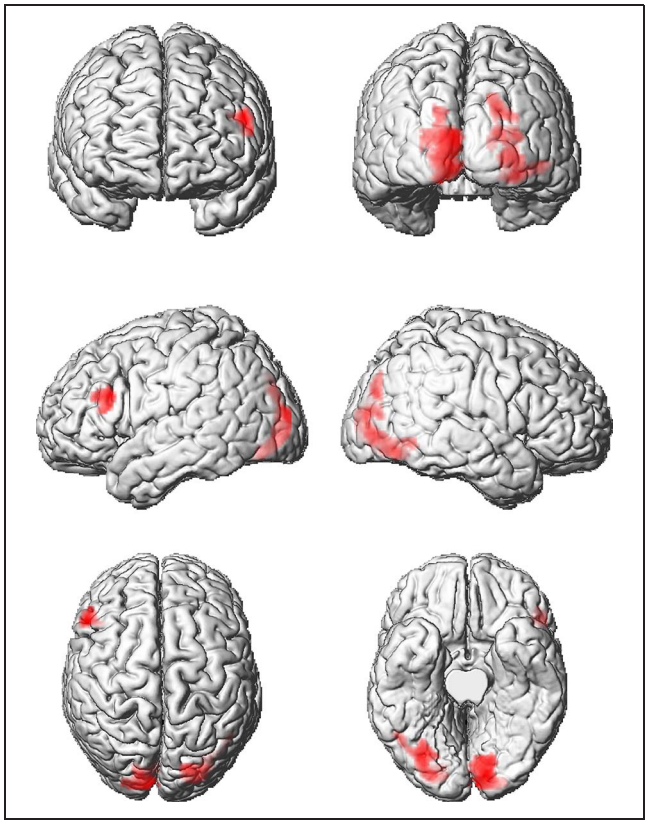

Figure 3. Surface renderings for the conjunction. Surface renderings for the conjunction of two contrasts, yielding activations that are higher for larger than smaller perceived size as caused by the two illusions.

Rescaling Size

Regions associated with a common but capacity-limited mechanism involved in rescaling perceived size in both illusions were identified using a functional contrast for the interaction. The contrast revealed areas associated with size adaptation in general, hence for both directions that were more active when the Ebbinghaus illusion was absent than when it was present [(adaptor present/Ebbinghaus absent − adaptor absent/Ebbinghaus absent) − (adaptor present/Ebbinghaus present − adaptor absent/Ebbinghaus present)]. On the basis of the behavioral data, this differential contrast did not reflect any net changes in perceived size. The contrast revealed three significant clusters (Table 2b, Figure 4): One cluster in the left occipital lobe expanded from the calcarine sulcus to the lingual and calcarine gyri. No activation was found in visual areas of the right hemisphere. In addition, two clusters in the right parietal cortex were identified: first, a cluster located in the supramarginal gyrus extending to the inferior postcentral gyrus and the rolandic operculum and, second, a cluster located in the superior parietal lobe encompassing the intraparietal sulcus and parts of the precuneus. Beta values extracted at the locations of the maximum *Z* score of the three clusters illustrated the nature of the interaction (Figure 5): The small adaptor (condition 2) led to less activation than the large adaptor (condition 3) when both adaptors were presented separately. This effect was reversed when the adaptors and the Ebbinghaus illusion were combined. In this case, the small adaptor (condition 5) led to more activation than the large adaptor (condition 6). Moreover, for the left visual cortex and the right SPL, trials with one illusion only (light gray dashed bars) had higher activation compared with trials during which the two illusions were presented simultaneously (light gray solid bars). During neutral trials (condition 1; dark gray bar), activation was lowest for all maxima, while activation was highest for the Ebbinghaus illusion presented alone (condition 4).

DISCUSSION

The current study shows that combining two visual illusions did not further modulate perceived size at the

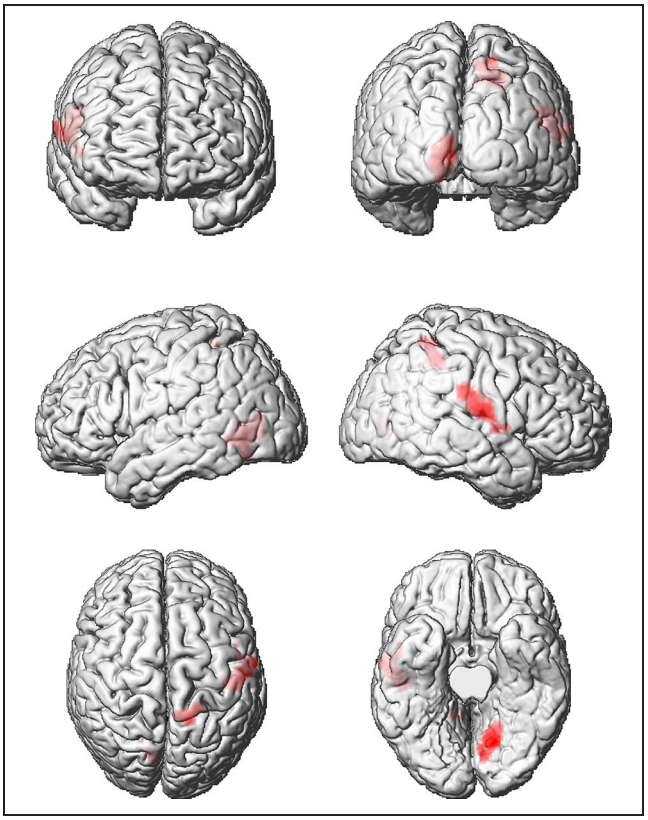

Figure 4. Surface renderings for the interaction. Surface renderings for the functional contrast testing for the interaction between the effect of the adaptors and the effect of the Ebbinghaus illusion, indicating activation associated with rescaling size in general.

behavioral level—neither did it induce functional activation beyond that induced by either illusion separately. These findings shed new light on the mechanisms underlying the generation of perceived size. Temporal separation of physical illusion inducers and test stimuli for the Ebbinghaus illusion and the size adaptation effect enabled identification of a common mechanism for rescaling perceived size in both illusions. Note that a successful separation of neural signals generated by the illusion-inducing adaptation display from those generated by the test stimuli allowed comparing size illusion effects specifically on test stimuli. Essentially, the test stimuli were physically identical across all experimental conditions irrespective of the preceding illusion inducers. Areas generally processing visual size illusions were identified by a global conjunction analysis. This contrast identified voxels where both illusions consistently decreased perceived size and where this effect was jointly significant.

Clusters around left IFG (pars triangularis) and bilateral occipital areas V1, V2, ventral V3 (V3v), and V4 were classified using the SPM anatomy toolbox (Eickhoff et al., 2005). The observed occipital activations support the hypothesis that early visual regions such as V1 encode changes in perceived size (Schwarzkopf et al., 2011; Fang et al., 2008; Murray et al., 2006). Left IFG, on the other hand, has previously been associated with a wide range of cognitive control tasks such as the selection of relevant information (Moss et al., 2005; Zhang, Feng, Fox, Gao, & Tan, 2004), interference resolution (Nelson, Reuter-Lorenz, Persson, Sylvester, & Jonides, 2009), task switching (Philipp, Weidner, Koch, & Fink, 2013; Dove, Pollmann, Schubert, Wiggins, & von Cramon, 2000), and response inhibition (Swick, Ashley, & Turken, 2008).

Taken together, left IFG and, in particular, the part of the pars triangularis corresponding to BA 45 seem to be activated whenever there is a need to select between competing processes or competing representations (for a review, see Badre & Wagner, 2007). This is also true for representations of numerosity. For instance, left IFG

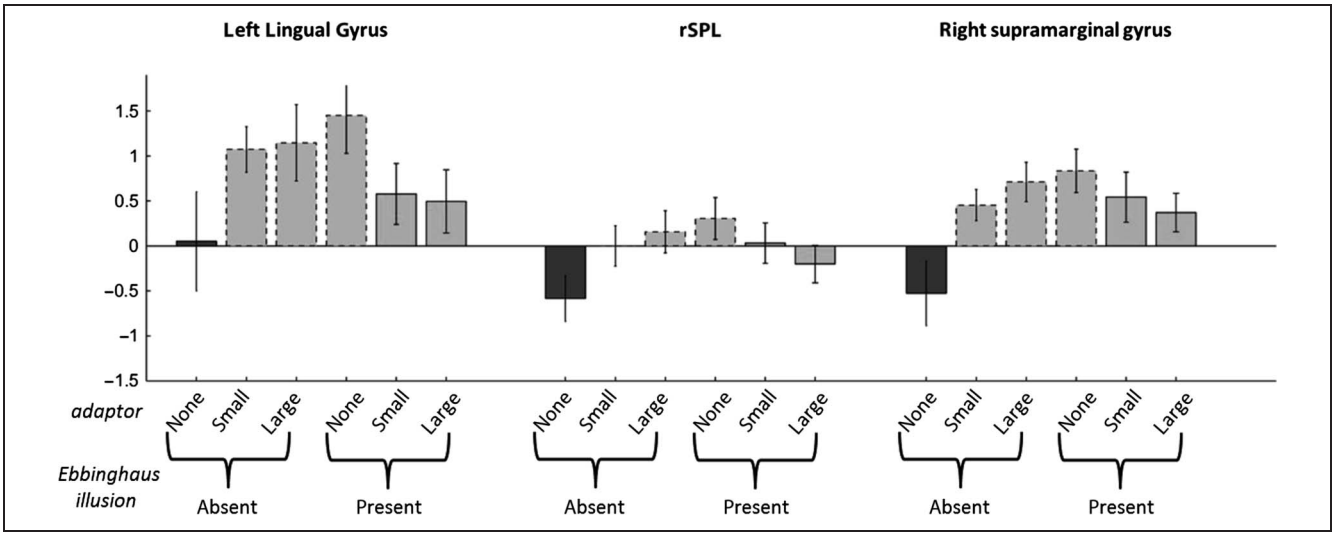

Figure 5. Bar graphs of the extracted beta values. The figure illustrates the beta values for the local maxima within the three clusters that were identified for the interaction contrast. The dark gray bars represent the neutral condition, whereas dashed light gray bars illustrate conditions with one illusion only. The solid light gray bars represent conditions where two illusions were presented simultaneously.

activation was observed when participants were asked to judge the numerosity of a dot pattern while at the same time ignoring their overall shape (Fink et al., 2001). In our study, left IFG was activated when participants perceived a circle as larger indicating a possible involvement in selecting a particular size representation.

Because the conjunction analysis revealed areas consistently activated by changes in perceived size, irrespective of whether these were caused by the Ebbinghaus illusion or by size adaptation, the activated areas are unspecific regarding the source of size changes and are most likely involved neither in generating perceived changes nor in explicit size judgments. Rather, these findings confirm previous reports on early visual involvement in coding perceived size (Schwarzkopf et al., 2011; Fang et al., 2008; Murray et al., 2006) and suggest that left IFG is involved in interference resolution between probe and target size.

To identify a putative central size-scaling module in form of a bottleneck with limited capacity, the interaction between the two illusions was investigated. At the behavioral level, the significant interaction was reflected by the fact that combining the Ebbinghaus illusion and the decreasing size adaptation led to illusion effects that did not differ from those elicited by both illusions separately. Such a limit in decreasing perceived size could theoretically result from an overriding feed-forward input to V1 as previously suggested by Murray et al. (2006). In this study, however, illusion-inducing stimuli and target circles were temporally separated, and the physical input to V1 was kept constant. The most parsimonious explanation for our behavioral findings could then be a capacity limitation of higher level processing: Such a limitation in decreasing perceived size may arise from a rescaling mechanism common to both illusions most likely based on top–down modulation from higher visual areas. The function of such a rescaling mechanism may be to integrate information about context over time and space and to generate rescaling parameters.

At the functional level, this mechanism was identified using fMRI. Here, the interaction contrast revealed regions that showed higher activation in response to any size adaptor when the Ebbinghaus illusion was absent as compared with times when the Ebbinghaus illusion was present. Importantly, behavioral data showed that this contrast did not imply noteworthy differences in PSEs. Note that this suggests that the activation cannot reflect any changes in size perception but instead must be attributed solely to context integration and the rescaling process itself. In this context, three significant clusters were identified, being located within left visual cortex (V1, V2, V3v, and V4), right supramarginal gyrus (rSMG), and right SPL. V1 has been shown before to be crucially involved in generating a subjective percept of visual size (Schwarzkopf & Rees, 2013; Sperandio, Chouinard, & Goodale, 2012; Schwarzkopf et al., 2011; Fang et al., 2008; Murray et al., 2006), and this was shown again by the conjunction analysis in the current study. However, the fact that V1 activation was also revealed by the interaction shows that it does not simply encode the results of a rescaling process but is crucially involved in generating it. Furthermore, V2, V3v, and V4 are hypothesized to play an important role in (relative) size perception by changing perceived size based on context information. Hereby, the different extrastriate visual cortices may serve different functions. One function is the estimation of an object's distance, which is important for forming size-constant object representations. A key mechanism involved in estimating object distance is relative disparity, and studies have shown that relative disparity is encoded along visual cortices V1, V2, and V4, gradually shifting from absolute to relative disparity (Umeda, Tanabe, & Fujita, 2007; Thomas, Cumming, & Parker, 2002). Given that (a) disparity is encoded in the most relative fashion at the level of V4 and (b) V4 is known to be essential for the integration of context for other features such as color constancy (Wild, Butler, Carden, & Kulikowski, 1985), it is reasonable to assume that V4 neurons may also "contribute to size constancy by systematically changing their size tuning depending on the viewing distance from objects" (Roe et al., 2012, p. 18). Furthermore, functional data on the neural correlates of the moon illusion suggest that V3v integrates retinal size and context information (Weidner et al., 2014).

Closer inspection of the beta values within the three clusters identified by the interaction showed that—at least with regard to rSPL and visual cortex—one illusion alone elicited more activation than the two illusions presented together. It appears that two simultaneous size-scaling processes may interfere with each other. This pattern shows that the capacity to integrate context and to perform size scaling within these regions is limited, suggesting that the identified network constitutes a bottleneck in illusion processing. Both the behavioral as well as functional data support this hypothesis as the combination of two illusions neither further decreased perceived size nor induced higher activation than both illusions did separately. Conclusively, the interaction contrast reveals a bottleneck network where the two illusions compete for processing resources with limited capacities.

Nevertheless, the functional role of the three clusters may differ. For instance, right SPL activation as identified by the interaction is presumably not necessary for illusion generation in general. This assumption is based on prior studies investigating the Müller–Lyer illusion, which have shown that, although the same cluster in right SPL is involved in using illusion information for further processing when it is task relevant (Weidner & Fink, 2007), its disruption by TMS does not interfere with the illusion generation per se (Mancini et al., 2010).

Taken together, the most parsimonious explanation of the data is that the role of the right SPL is to actively use the illusion information for judgments and comparisons after the illusion has been generated. The generation of the illusion must thus occur either within the rSMG or visual cortex or alternatively within both. Assuming that

the generation of the Ebbinghaus illusion and the size adaptation effect is processed similarly to the Müller–Lyer illusion, the possibility that the visual cortex is not involved in illusion generation is unlikely. It was already shown that occipital areas were necessary for illusion generation (Mancini et al., 2010). Therefore, the question is whether rSMG is involved in illusion generation together with the occipital areas or whether it receives output from visual occipital areas for further processing similar to the rSPL. In the light of an MEG study investigating the time course of the Müller–Lyer illusion (Weidner, Boers, Mathiak, Dammers, & Fink, 2010), the latter seems more plausible: Participants were presented with three different line arrangements that induced either one of two versions of the Müller–Lyer illusion or no illusion. Source reconstruction revealed stronger activation for illusion displays (compared with no illusion) spreading along the visual areas (85–195 msec after stimulus onset) to right inferior temporal gyrus (195–215 msec), supramarginal gyrus (260 msec), and IFG (395 msec). Illusion-related representations were taken to first become formed in the ventral visual pathway and subsequently to be processed in parietal cortex. Taken together, from the three clusters identified to be the bottleneck in processing the Ebbinghaus illusion and the size adaptation effect, only the visual areas seem to generate the illusion representation itself and rescale perceived size. Right parietal areas (rSPL and rSMG) receive the output and further process the illusion for the task at hand. In this study, activation of those two areas is likely to reflect the difficulty of size judgments when one or two illusions manipulate the size of one circle.

In summary, the current study shows that illusion processing and rescaling retinal into perceived size is constrained by capacity-limited common resources. However, with regard to the Ebbinghaus illusion, only underestimation of perceived size could be studied, and future research should investigate whether the same common resources are involved in other illusions allowing for size modulation in both directions. These common resources consist of left occipital areas V1, V2, V3v, and V4 as well as two clusters within the right parietal cortex, namely, SMG and SPL. Taking into account previous studies, the parietal activations are likely to reflect the use of updated size information for further task-related processing. The visual areas, on the other hand, constitute a bottleneck for size-scaling processes. Accordingly, a central size-scaling module can be identified within occipital cortex, albeit slightly more medially than the hypothesized candidate area within LOC, which has been found to be involved in the Müller–Lyer illusion.

Acknowledgments

R. W. is supported by the Deutsche Forschungsgemeinschaft (DFG, WE 4299/2-1). We are grateful to our colleagues from the Institute of Neuroscience and Medicine for many valuable discussions and help with MR scanning and to Kai V. Thilo for his helpful advice on a previous version of the manuscript. Additional support to G. R. F. from the Marga and Walter Boll Foundation is gratefully acknowledged.

Reprint requests should be sent to Sylvia Kreutzer, Cognitive Neuroscience, Institute of Neuroscience and Medicine, INM-3, Research Center Jülich, 52425 Jülich, Germany, or via e-mail: sy.kreutzer@fz-juelich.de.

REFERENCES

Badre, D., & Wagner, A. D. (2007). Left ventrolateral prefrontal cortex and the cognitive control of memory. *Neuropsychologia, 45,* 2883–2901.

Bullier, J. (2001). Integrated model of visual processing. *Brain Research Reviews, 36,* 96–107.

Busch, A., & Müller, H. J. (2004). The Ebbinghaus illusion modulates visual search for size-defined targets: Evidence for preattentive processing of apparent object size. *Perception & Psychophysics, 66,* 475–495.

Cooper, L. A., & Weintraub, D. J. (1970). Delboeuf-type circle illusions: Interactions among luminance, temporal characteristics, and inducing-figure variations. *Journal of Experimental Psychology, 85,* 75–82.

Dove, A., Pollmann, S., Schubert, T., Wiggins, C. J., & von Cramon, Y. D. (2000). Prefrontal cortex activation in task switching: An event-related fMRI study. *Cognitive Brain Research, 9,* 103–109.

Eickhoff, S. B., Stephan, K. E., Mohlberg, H., Grefkes, C., Fink, G. R., Amunts, K., et al. (2005). A new SPM toolbox for combining probabilistic cytoarchitectonic maps and functional imaging data. *Neuroimage, 25,* 1325–1335.

Fang, F., Boyaci, H., Kersten, D., & Murray, S. O. (2008). Attention-dependent representation of a size illusion in human V1. *Current Biology, 18,* 1707–1712.

Fink, G. R., Marshall, J. C., Gurd, J., Weiss, P. H., Zafiris, O., Shah, N. J., et al. (2001). Deriving numerosity and shape from identical visual displays. *Neuroimage, 13,* 46–55.

Friston, K. J., Penny, W. D., & Glaser, D. E. (2005). Conjunction revisited. *Neuroimage, 25,* 661–667.

Jaeger, T., & Pollack, R. H. (1977). Effect of contrast level and temporal order on the Ebbinghaus circles illusion. *Perception & Psychophysics, 21,* 83–87.

Libedinsky, C., & Livingstone, M. (2011). Role of prefrontal cortex in conscious visual perception. *Journal of Neuroscience, 31,* 64–69.

Lumer, E. D., & Rees, G. (1999). Covariation of activity in visual and prefrontal cortex associated with subjective visual perception. *Proceedings of the National Academy of Sciences, U.S.A., 96,* 1669–1673.

Macmillan, N. A., & Creelman, C. D. (1991). Adaptive methods for estimating empirical thresholds. In N. A. Macmillan & C. D. Creelman (Eds.), *Detection theory: A user's guide* (pp. 183–209). Cambridge: Cambridge University Press.

Mancini, F., Bolognini, N., Bricolo, E., & Vallar, G. (2010). Cross-modal processing in the occipito-temporal cortex: A TMS study of the Müller-Lyer illusion. *Journal of Cognitive Neuroscience, 23,* 1987–1997.

Moss, H. E., Abdallah, S., Fletcher, P., Bright, P., Pilgrim, L., Acres, K., et al. (2005). Selecting among competing alternatives: Selection and retrieval in the left inferior frontal gyrus. *Cerebral Cortex, 15,* 1723–1735.

Murray, S. O., Boyaci, H., & Kersten, D. (2006). The representation of perceived angular size in human primary visual cortex. *Nature Neuroscience, 9,* 429–434.

Nelson, J. K., Reuter-Lorenz, P. A., Persson, J., Sylvester, C.-Y. C., & Jonides, J. (2009). Mapping interference resolution across

task domains: A shared control process in left inferior frontal gyrus. *Brain Research, 1256,* 92–100.
Oldfield, R. C. (1971). The assessment and analysis of handedness: The Edinburgh inventory. *Neuropsychologia, 9,* 97–113.
Philipp, A. M., Weidner, R., Koch, I., & Fink, G. R. (2013). Differential roles of inferior frontal and inferior parietal cortex in task switching: Evidence from stimulus-categorization switching and response-modality switching. *Human Brain Mapping, 34,* 1910–1920.
Plewan, T., Weidner, R., Eickhoff, S. B., & Fink, G. R. (2012). Ventral and dorsal stream interactions during the perception of the Müller–Lyer illusion: Evidence derived from fMRI and dynamic causal modeling. *Journal of Cognitive Neuroscience, 24,* 2015–2029.
Plewan, T., Weidner, R., & Fink, G. R. (2012). The influence of stimulus duration on visual illusions and simple reaction time. *Experimental Brain Research, Experimentelle Hirnforsch Expérimentation Cérébrale, 223,* 367–375.
Pooresmaeili, A., Arrighi, R., Biagi, L., & Morrone, M. C. (2013). Blood oxygen level-dependent activation of the primary visual cortex predicts size adaptation illusion. *Journal of Neuroscience, 33,* 15999–16008.
Roe, A. W., Chelazzi, L., Connor, C. E., Conway, B. R., Fujita, I., Gallant, J. L., et al. (2012). Toward a unified theory of visual area V4. *Neuron, 74,* 12–29.
Schwarzkopf, D. S., & Rees, G. (2013). Subjective size perception depends on central visual cortical magnification in human V1. *PLoS One, 8,* e60550.
Schwarzkopf, D. S., Song, C., & Rees, G. (2011). The surface area of human V1 predicts the subjective experience of object size. *Nature Neuroscience, 14,* 28–30.
Sperandio, I., Chouinard, P. A., & Goodale, M. A. (2012). Retinotopic activity in V1 reflects the perceived and not the retinal size of an afterimage. *Nature Neuroscience, 15,* 540–542.
Sperandio, I., Lak, A., & Goodale, M. A. (2012). Afterimage size is modulated by size-contrast illusions. *Journal of Vision, 12*. doi: 10.1167/12.2.18.
Swick, D., Ashley, V., & Turken, A. U. (2008). Left inferior frontal gyrus is critical for response inhibition. *BMC Neuroscience, 9,* 102.
Thomas, O. M., Cumming, B. G., & Parker, A. J. (2002). A specialization for relative disparity in V2. *Nature Neuroscience, 5,* 472–478.
Umeda, K., Tanabe, S., & Fujita, I. (2007). Representation of stereoscopic depth based on relative disparity in macaque area V4. *Journal of Neurophysiology, 98,* 241–252.
Weidner, R., Boers, F., Mathiak, K., Dammers, J., & Fink, G. R. (2010). The temporal dynamics of the Müller–Lyer illusion. *Cerebral Cortex, 20,* 1586–1595.
Weidner, R., & Fink, G. R. (2007). The neural mechanisms underlying the Müller–Lyer illusion and its interaction with visuospatial judgments. *Cerebral Cortex, 17,* 878–884.
Weidner, R., Plewan, T., Chen, Q., Buchner, A., Weiss, P. H., & Fink, G. R. (2014). The moon illusion and size-distance scaling—Evidence for shared neural patterns. *Journal of Cognitive Neuroscience, 26,* 1871–1882.
Wild, H. M., Butler, S. R., Carden, D., & Kulikowski, J. J. (1985). Primate cortical area V4 important for colour constancy but not wavelength discrimination. *Nature, 313,* 133–135.
Zhang, J. X., Feng, C.-M., Fox, P. T., Gao, J.-H., & Tan, L. H. (2004). Is left inferior frontal gyrus a general mechanism for selection? *Neuroimage, 23,* 596–603.